frontiers in Materials

ORIGINAL RESEARCH
published: 08 April 2021
doi: 10.3389/fmats.2021.664220

Nanoindentation of Nanoglasses Tested by Molecular Dynamics Simulations: Influence of Structural Relaxation and Chemical Segregation on the Mechanical Response

Omar Adjaoud and Karsten Albe*

Fachbereich Material- und Geowissenschaften, Fachgebiet Materialmodellierung, Technische Universität Darmstadt, Darmstadt, Germany

OPEN ACCESS

Edited by:
Shiv Prakash Singh, International Advanced Research Centre for Powder Metallurgy and New Materials, India

Reviewed by:
Yunjiang Wang, Chinese Academy of Sciences, China
Indrasen Singh, Indian Institute of Technology Indore, India

***Correspondence:**
Omar Adjaoud
adjaoud@mm.tu-darmstadt.de

Specialty section:
This article was submitted to Ceramics and Glass, a section of the journal Frontiers in Materials

Received: *04 February 2021*
Accepted: *15 March 2021*
Published: *08 April 2021*

Citation:
Adjaoud O and Albe K (2021) Nanoindentation of Nanoglasses Tested by Molecular Dynamics Simulations: Influence of Structural Relaxation and Chemical Segregation on the Mechanical Response. Front. Mater. 8:664220. doi: 10.3389/fmats.2021.664220

We present molecular dynamics simulations of nanoindentation in order to investigate the effects of segregation and structural relaxation on the mechanical properties of $Cu_{64}Zr_{36}$ nanoglasses prepared by particle consolidation and long-time annealing. Our analysis of load-displacement curves shows that the effective elastic modulus of nanoglasses is lower than that of their homogeneous metallic glass counterpart. This is mainly because of the defective short-range order present in the glass-glass interface, but to a lesser extend due to chemical inhomogeneities. Structural relaxation obtained by long-time annealing (500 ns) at 0.8 T_g leads to a shift from a homogeneous deformation to a mix of homogeneous deformation and shear bands. The obtained hardness values of annealed nanoglass are comparable to those of homogenous glass samples, but significantly higher as compared to juvenile as-prepared nanoglass samples. The results are discussed in the context of recent nanonindentation experiments.

Keywords: metallic glass, nanoglass, glass-glass interfaces, structural relaxation, segregation, nanoindentation, mechanical properties, molecular dynamics

1. INTRODUCTION

Metallic nanoglasses are non-crystalline solids, which can be synthesized by cold-compaction of nanometer-sized metallic glassy particles obtained from inert gas condensation (Jing et al., 1989; Weissmüller et al., 1992; Gleiter, 2008, 2013, 2016; Fang et al., 2012; Gleiter et al., 2014; Nandam et al., 2017; Ivanisenko et al., 2018). The microstructure of nanoglasses consists of glassy grains connected by glass-glass interfaces (Ritter et al., 2011; Ivanisenko et al., 2018). These interfacial regions are characterized by an excess volume (Jing et al., 1989; Şopu et al., 2009), a defective short–range order (SRO) (Ritter et al., 2011), and a different composition as compared to the grain interiors (Adjaoud and Albe, 2016, 2018; Wang C. et al., 2016; Nandam et al., 2017, 2020).

In order to see whether nanoglasses have superior mechanical properties over their metallic glass counterparts, several experimental studies of Fe-Sc, Cu-Zr, and Pd-Si nanoglasses were conducted in the past (Franke et al., 2014; Nandam et al., 2017, 2020; Arnold et al., 2020; Sharma et al., 2021). Ultrasonic measurements of $Fe_{86}Sc_{14}$, $Fe_{90}Sc_{10}$, $Cu_{58}Zr_{42}$, and $Cu_{60}Zr_{40}$ nanoglasses showed that

their Young's moduli are lower than those of the homogenous metallic glass counterparts (Arnold et al., 2020), which is in line with results obtained by nanoindentation of $Fe_{90}Fe_{10}$ and $Pd_{80}Si_{20}$ nanoglasses (Franke et al., 2014; Nandam et al., 2017, 2020). The lower stiffness of the nanoglasses were attributed to sample porosity by Arnold et al. (2020). Nanoindentation of $Sc_{75}Fe_{25}$ and $Cu_{50}Zr_{50}$, in contrast, revealed that Young's moduli and hardness values of these nanoglasses are higher than those of the metallic glasses with identical chemical composition (Franke et al., 2014; Nandam et al., 2017, 2020). This was explained by segregation effects and the resulting different chemical bonding in the interfaces (Nandam et al., 2020).

As it comes to the yielding mechanism, shear bands were observed in uniaxial microcompression tests and nanoindentation of $Pd_{80}Si_{20}$ nanoglasses (Nandam et al., 2020; Sharma et al., 2021), while similar experimental tests of $Sc_{75}Fe_{25}$, $Cu_{50}Zr_{50}$, and $Cu_{60}Zr_{40}$ nanoglasses revealed that these nanoglasses deform homogeneously (Fang et al., 2012; Wang et al., 2015; Wang X. et al., 2016; Nandam et al., 2017; Sharma et al., 2021).

It is widely accepted that the plastic deformation of (bulk) metallic glasses is carried by shear transformation zones (STZs) which are clusters of atoms in the glassy structure that undergo a cooperative reorganization upon application of stress (Argon, 1979; Schuh et al., 2007). The distribution of STZs can lead to a homogeneous deformation or to the formation of shear bands, depending on the structural state of a metallic glass, the temperature, and the applied strain rate (Schuh et al., 2007). Structural relaxation of metallic glasses by annealing below their glass transition temperature,T_g, leads to annihilation of free volume and changes of the topological SRO (Schuh et al., 2007), which, consequently, affects its mechanical properties (Lee K. S. et al., 2007; Yoo et al., 2009; Choi et al., 2012).

Molecular dynamics (MD) simulations of uniaxial loading tests revealed that glass-glass interfaces in nanoglasses and the glass-crystal interfaces in nanoglass-crystal composites promote the activity of STZs (Şopu et al., 2011; Adibi et al., 2013; Albe et al., 2013; Şopu and Albe, 2015; Kalcher et al., 2017a,b, 2020; Adjaoud and Albe, 2019, 2020; Cheng and Trelewicz, 2019b). The mechanical response of nanoglasses tested by nanoindentation, however, has not been subject of simulation studies, yet.

In the present work, we study nanoindentation of $Cu_{64}Zr_{36}$ nanoglasses by molecular dynamics simulations. We investigate the influence of chemical segregation to the glass-glass interfaces and the effects of structural relaxation by comparing as-prepared and annealed nanoglasses.

2. METHODOLOGY

In this study, we employed molecular dynamics simulations using the LAMMPS simulation package (Plimpton, 1995). Interatomic interactions are described by an embedded atom model (EAM) potential for Cu-Zr (Mendelev et al., 2009). This potential has been optimized to predict accurately the structure of liquid and amorphous Cu-Zr alloys and was successfully applied to identify the deformation mechanisms in Cu-Zr glasses (Tang and Harrowell, 2013; Lee et al., 2015; Zemp et al., 2015). In all simulations the equations of motion were numerically integrated with a time step of 2 fs. Temperature and pressure were controlled by Nosé-Hoover thermostat and barostat, as implemented in LAMMPS (Plimpton, 1995). Homogeneous glass and nanoglass samples were prepared using 3-dim. periodic boundary conditions.

For obtaining a juvenile homogenous glass, a melt was equilibrated at 2,000 K and then quenched to the glassy state (50 K) using a cooling rate of 0.01 K ps^{-1}. The atomic structure of the prepared $Cu_{64}Zr_{36}$ glass shows good agreement with previous studies (Ritter et al., 2011; Cheng et al., 2013; Ding et al., 2014; Zemp et al., 2015; Adjaoud and Albe, 2016; Kalcher et al., 2017b). The $Cu_{64}Zr_{36}$ nanoglass was obtained by cold compaction of several glassy spheres with diameter ranging from 6 to 8 nm. Full details of the preparation of the nanoglass can be found in Adjaoud and Albe (2018). The resulting NG have dimensions of about 18 × 18 × 18 nm and their microstructures consist of glassy regions connected by glass-glass interfaces. These interfaces are characterized by a defective SRO in a zone with a width of at least 2 nm (Adjaoud and Albe, 2018; Cheng and Trelewicz, 2019a). In terms of composition, the $Cu_{64}Zr_{36}$ nanoglass is composed of slightly Cu-deficient glassy bulk regions ($Cu_{61}Zr_{39}$) and Cu-rich interfaces ($Cu_{72}Zr_{28}$) extending over about 1 nm, as shown in **Figure 1**: red and blue colors are atoms in the glassy regions; green and yellow colors are atoms in the interfaces. The chemical segregation at the interfaces results from surface segregation effects in the primary glassy spheres (Adjaoud and Albe, 2016; Wang C. et al., 2016).

In order to see whether chemical segregation affects the mechanical properties of nanoglasses during nanoindentation, we studied a chemically homogenous nanoglass for comparison. We prepared the non-segregated, chemically homogenous nanoglass by consolidating several compositionally homogeneous glassy spheres. The glassy spheres were equilibrated at a temperature of 50 K, where the kinetics is slow, and thus the glassy spheres remained compositionally homogeneous (Adjaoud and Albe, 2018, 2019).

For studying the effect of structural relaxation on mechanical properties, the homogeneous glass and nanoglass samples were subsequently annealed at 600 K ($\approx 0.8T_g$) for 500 ns. This annealing time is much longer than those used in previous MD simulations of nanoglasses which was 70 ns the longest (Ritter et al., 2011; Şopu et al., 2011; Cheng and Trelewicz, 2019b).

For nanoindentation simulations, the homogeneous glasses and nanoglasses were replicated and relaxed in order to construct larger samples with dimensions of 18 × 72 × 36 nm (see **Figure 1**). We followed the same procedure as the one described in previous MD nanoindentation simulations (Shi and Falk, 2007; Deng and Schuh, 2012). Two-dimensional periodic boundary conditions were applied, while one surface was exposed to the nanoindenter. In order to avoid the translation of the center of mass of the whole sample during nanoindentation, atoms in a layer with a width of about 2 nm at the bottom along Z direction were fixed. Nanoindentation simulations were performed by using a virtual cylindrical indenter with a radius, R of 20 nm (**Figure 1**). The virtual cylindrical indenter exerts a repulsive

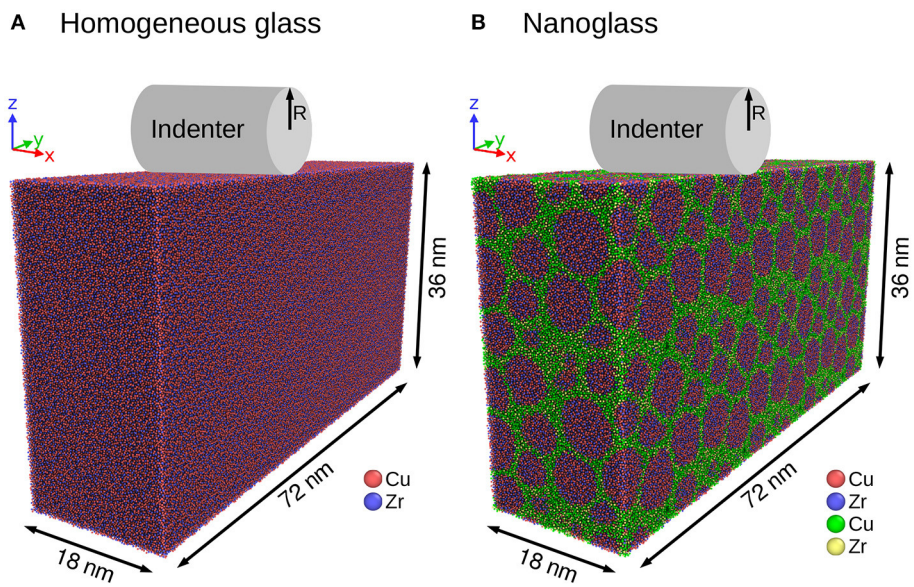

FIGURE 1 | Nanoindentation simulation models for **(A)** homogeneous glass and **(B)** nanoglass. The radius of the virtual cylindrical indenter, R, is 20 nm. Homogeneous glass is compositionally homogeneous, while nanoglass is compositionally heterogeneous. Color scheme is indicating regions with deviation in composition. The average grain size of the nanoglass is about 7 nm.

force with a magnitude of $p(r) = K(r-R)^2$, where r is the distance from the atom to the center of the indenter and $K = 100\,\text{eV}/\text{Å}^3$ is the specified force constant. Nanoindentation simulations are conducted in displacement-controlled mode with a rate of 1 m/s. The maximum indentation depth is 5 nm. Each nanoindentation simulation is carried out in three steps: loading, holding at the maximum indentation depth, and unloading.

For determining the effective elastic modulus (E_{eff}) and the hardness (H), we applied the Oliver Pharr approach (Oliver and Pharr, 2004). Here, the $p - h$ curve is used in order to determine the mechanical properties of a material, while the Young's modulus and hardness are calculated using the following relations (Oliver and Pharr, 2004),

$$E_{eff} = \frac{S}{2}\sqrt{\frac{\pi}{A_c}}, \tag{1}$$

and

$$H = \frac{P_{max}}{A_c}, \tag{2}$$

where $S = (dp/dh)_{h=h_{max}}$ is the elastic unloading stiffness, which is defined as the slope of the unloading curve at $h = h_{max}$. The unloading curve is described by the power-law relation,

$$P = \alpha(h - h_f)^m, \tag{3}$$

where α is a fitting parameter. For describing an indenter with a paraboloid of revolution we have chosen $m = 1.5$ (Oliver and Pharr, 2004). This value is consistent with previous MD simulations (Deng and Schuh, 2012). The final depth after unloading is h_f. P_{max} is the maximum load. A_c is the contact area which is defined from the geometry of the indenter,

$$A_c = 2L_x\sqrt{h_c(2R - h_c)}, \tag{4}$$

where $L_x = 18$ nm is the length of the cylindrical indenter. The contact depth h_c is given by the relation (Oliver and Pharr, 2004)

$$h_c = h_{max} - 0.75\frac{P_{max}}{S}. \tag{5}$$

The atomic scale deformation mechanisms were analyzed in terms of the local atomic von Mises shear strain (Falk and Langer, 1998; Shimizu et al., 2007) calculated with the OVITO analysis and visualization software (Stukowski, 2010).

3. RESULTS

3.1. Model Structures Before and After Annealing

In order to quantify the structural features present in the various model glasses before indentation, we calculated the fraction of Cu-centered full icosahedra (Cu [0,0,12,0]). They are characterized by a high packing density (Lee J. C. et al., 2007) as well as high shear resistance (Cheng et al., 2008) and are known to be the key structural units in $Cu_{64}Zr_{36}$ metallic glasses.

Figure 2 presents the results for the grain interior and interfaces of as-prepared and annealed $Cu_{64}Zr_{36}$ nanoglasses. Non-segregated and segregated nanoglasses as well as juvenile and annealed homogeneous glass are considered. In the interfaces of as-prepared nanoglasses the icosahedra fractions are significantly lower than those in the grain interiors, confirming

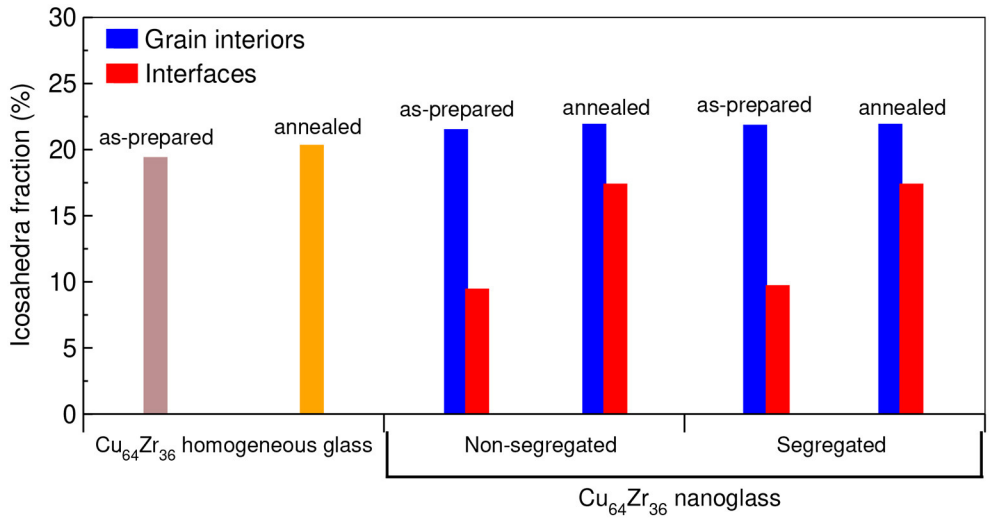

FIGURE 2 | Fraction of Cu-centered full icosahedra in the grain interiors and interfaces of the as-prepared and annealed $Cu_{64}Zr_{36}$ non-segregated and segregated nanoglasses. As-prepared and annealed homogeneous glasses with identical chemical composition are shown for comparison. Annealing is performed at a temperature of 600 K (≈0.8T_g) for 500 ns.

that the interfaces are characterized by a defective SRO (Ritter et al., 2011; Adjaoud and Albe, 2018, 2019; Cheng and Trelewicz, 2019a). After annealing there is little change in the homogeneous glass and the grain interiors of the nanoglasses, whereas significant structural recovery can be seen in the interfacial areas of both types of nanoglasses where the icoshedra content is increasing. However, even by the long-time annealing treatment (500 ns) the interfaces do not fully recover, as the icosahedra fraction is still lower than in the grain interiors. These results confirm that the microstructure of nanoglasses is stable if the annealing temperature stays below T_g. This is consistent with previous MD simulations and experimental results (Ritter et al., 2011; Şopu et al., 2011; Franke et al., 2014; Cheng and Trelewicz, 2019b) and is analogous to shear bands. These are also structurally distorted planar defects, which do no recover by thermal annealing below T_g.

Previous MD results on uniaxial tensile deformation of $Cu_{64}Zr_{36}$ nanoglasses showed that the mechanical properties of nanoglasses are strongly correlated with the icosahedra fraction (Adjaoud and Albe, 2019; Cheng and Trelewicz, 2019b). Since the as-prepared non-segregated and segregated nanoglasses exhibit about the same fraction of icosahedra the mechanical properties probed by nanoindentation are expected to be similar if the segregation doesn't affect the local stiffness.

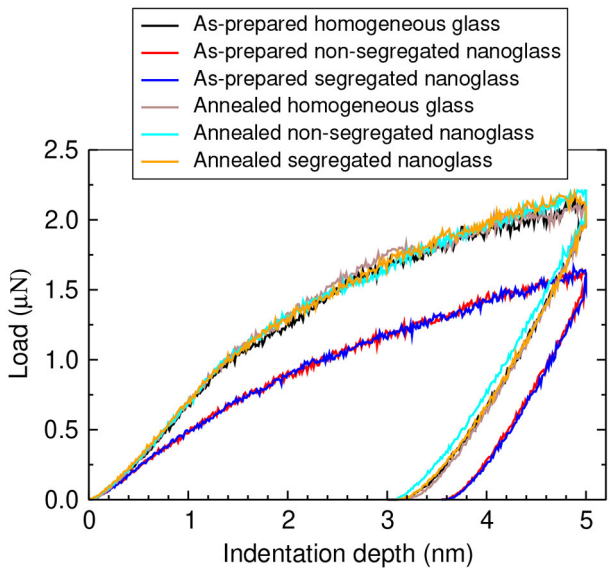

FIGURE 3 | P-h curves during nanoindentation of the as-prepared and annealed $Cu_{64}Zr_{36}$ non-segregated and segregated nanoglasses. As-prepared and annealed homogeneous glasses with identical chemical composition are added for comparison.

3.2. Effective Elastic Modulus and Hardness

In the following we address the question whether segregation and structural relaxation influence the response of nanoglasses on nanoindentation. In doing so, we monitored the load as a function of indentation depth. **Figure 3** shows load-displacement (P-h) curves for as-prepared and annealed samples. It can clearly be seen, that the mechanical response of all samples can be divided into two classes: the as-prepared nanoglasses, both segregated and non-segregated, show a much softer response. The homogenous bulk glasses and annealed nanoglasses, however, exhibit the same response and require significantly larger loads. This is in agreement with nanoindentation experiments on $Cu_{50}Zr_{50}$ nanoglasses (Nandam et al., 2017) and can be explained by the increasing fraction of icosahedra

TABLE 1 | Effective elastic modulus and hardness obtained by nanoindentation of as-prepared and annealed samples.

Samples	As-prepared		Annealed	
	Effective elastic modulus (GPa)	Hardness (GPa)	Effective elastic modulus (GPa)	Hardness (GPa)
Homogeneous glass	66.8	4.7	68.3	4.6
Non-segregated nanoglass	66.1	3.4	66.0	4.8
Segregated nanoglass	64.4	3.3	66.4	4.5

after annealing (see **Figure 2**). Notably, there is only marginal differences between segregated and non-segregated nanoglasses, which implies that chemical inhomogeneities on that length scale have little impact on the critical stress needed for STZ activation. These finding are also in line with previous MD results on tensile deformation of $Cu_{64}Zr_{36}$ nanoglasses, which showed that the deformation behavior of nanoglasses is controlled by the defective SRO in the interfaces rather than by the composition of the interfaces (Adjaoud and Albe, 2019). In a next step, we calculated elastic unloading stiffness and hardneess (Equations 1 and 2) of as-prepared and annealed samples. The obtained results are summarized in **Table 1**. The effective elastic modulus of the homogenous glass is in agreement with previous results using the same interatomic potential (Deng and Schuh, 2012) and slightly higher than that of the nanoglasses, which can be attributed to the presence of softer glass-glass interfaces. After annealing the stiffness of all samples is increasing but the influence on the effective elastic modulus is quite small and the effective elastic moduli of as-prepared and annealed nanoglasses are still lower than that of the homogeneous glass.

A considerable effect, however, can be seen in the hardness values. The hardness of the nanoglasses increases significantly after annealing (≈41% in the non-segregated nanoglass and ≈36% in the segregated nanoglass); they reach the value of the homogeneous glass. Furthermore, the non-segregated and segregated nanoglasses show similar values for the effective elastic modulus and hardness, which is consistent with the fractions of icosahedra and $P-h$ curves presented in **Figures 2**, **3**.

Recent nanoindentation experiments on $Cu_{50}Zr_{50}$ nanoglasses showed that as-prepared and annealed nanoglasses have about the same effective elastic modulus and hardness. The $Cu_{50}Zr_{50}$ nanoglass was annealed at 350 °C ($\approx 0.9T_g$ of melt-spun ribbon) for 3 h (Nandam et al., 2017). This finding seems to be at odds to our simulations results. However, if we acknowledge that experimentally at ambient conditions structural relaxations can even occur before mechanical testing then the as-prepared juvenile state of virtual nanoglasses is not present in experimental samples and the annealing procedures has little impact on the defective short-range order (Nandam et al., 2020).

3.3. Strain Localization and Deformation Mechanisms

After we had seen that interfacial relaxation has a significant impact on the obtained hardness of nanoglasses we investigated the strain localization during nanoindentation. In doing so, we calculated the strain localization parameter as defined by Cheng et al. (2009), $\Psi = \sqrt{\frac{1}{N}\sum_{i=1}^{N}(\eta_i - \eta_{ave})^2}$, where N is the total number of atoms in the simulation box, η_i is the von Mises shear strain of atom i, and η_{ave} is the average of von Mises strain of all atoms. Ψ assesses the deviation of strain distribution from the homogeneous behavior: a larger Ψ value implies larger fluctuations in the atomic strain and a more localized deformation mode.

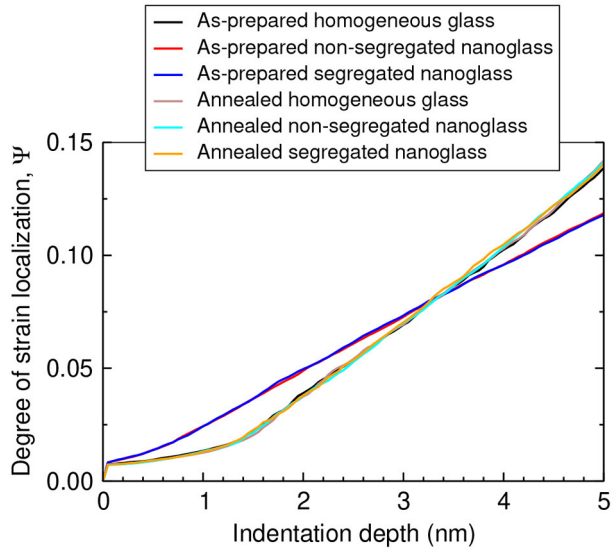

FIGURE 4 | The degree of strain localization parameter, ψ, during nanoindentation of the as-prepared and annealed $Cu_{64}Zr_{36}$ non-segregated and segregated nanoglasses. As-prepared and annealed homogeneous glasses with identical chemical composition are shown for comparison.

Figure 4 displays the variation of the Ψ parameter during nanoindentation of as-prepared and annealed samples. Again we see that as-prepared nanoglasses exhibit a different behavior as compared to all other samples, which is consistent with $P-h$ curves presented in **Figure 3**. At lower indentation depths, as-prepared nanoglasses have higher Ψ values because of the lower fraction of icosahedra in interfaces which facilitate shear activities in the interfacial regions. After annealing, the nanoglasses show a similar behavior as the homogeneous metallic glass, where the Ψ parameter displays an abrupt increase at an indentation depth of about 1.2 nm. Again, there is no difference between the non-segregated and segregated nanoglasses and the variation of the Ψ parameter during nanoindentation is almost identical.

For obtaining insights into the deformation mechanism of as-prepared and annealing samples below the indentation, we calculated the von Mises shear strain for each atom at the maximum indentation depth, 5 nm, which is presented in **Figure 5**, taking the undeformed samples as reference structures. In as-prepared and annealed homogeneous glasses, strain localization occurs in the form of a few shear bands underneath the indenter. Moreover, the plastic deformation is mainly carried by these shear bands. In the case of the nanoglasses, there

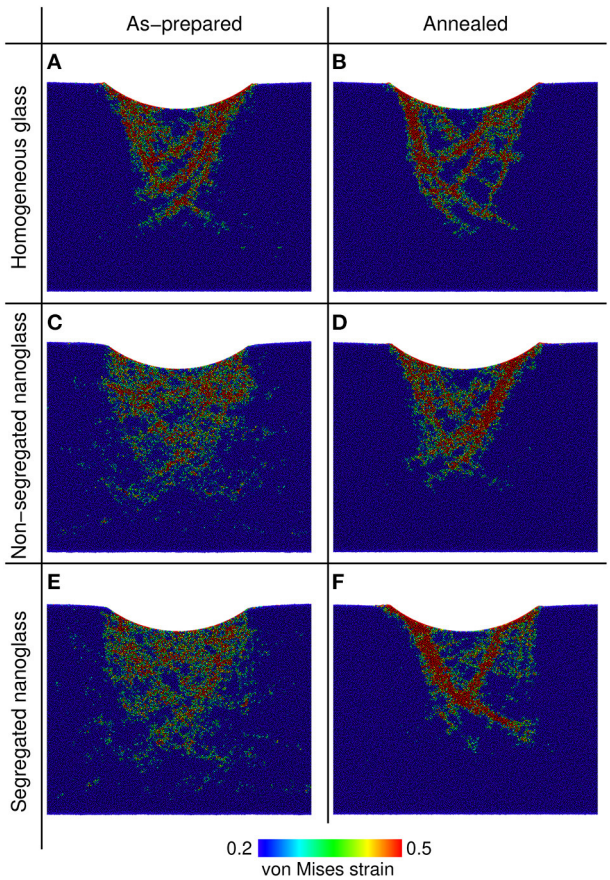

FIGURE 5 | Local atomic von Mises shear strain at indentation depth of 5 nm for **(C,E)** as-prepared and **(D,F)** annealed Cu64Zr36 non-segregated and segregated nanoglasses, as well **(A)** as-prepared and **(B)** annealed homogeneous glasses with identical chemical composition.

is an obvious difference on strain localization between as-prepared and annealed samples. Strain localization in the as-prepared nanoglasses is more homogeneous and the plastic deformation region is wider than in the annealed nanoglasses. This can be explained by the lower fraction of icosahedra (i.e., a defective SRO) in the interfaces of as-prepared nanoglasses, which decrease the activation barrier for STZs (Şopu et al., 2011; Albe et al., 2013; Şopu and Albe, 2015; Adjaoud and Albe, 2019; Cheng and Trelewicz, 2019b). The annealed nanoglasses show an intermediate strain localization behavior: the plastic deformation is carried not only by shear bands but also by some local deformations. These local deformations appear because the interfaces in nanoglasses still exist even after annealing (see **Figure 2**). Interestingly, while these differences are visible from the locally resolved von Mises strain, the global strain localization parameter presented in **Figure 4** is insensitive to these features.

4. DISCUSSION

Experimentally, nanoindendation of $Sc_{75}Fe_{25}$ and $Cu_{50}Zr_{50}$ nanoglasses showed higher Young's moduli and Hardness values as compared to the metallic glasses with identical chemical composition. The opposite tendency was observed for $Fe_{90}Fe_{10}$ and $Pd_{80}Si_{20}$ nanoglasses (Franke et al., 2014; Nandam et al., 2017, 2020). These differences in Young's moduli and Hardness values were indirectly attributed to the chemical segregation in the interfacial regions (Nandam et al., 2020). Our MD simulation results, in contrast, reveal that chemical segregation only slightly affects the mechanical properties of Cu-Zr nanoglasses, while the degree of ordering (i.e., fraction of icosahedra) in the interfaces has a significant influence on the Hardness values.

Contrary to the indentation experiments, recent ultrasonic measurements of Fe-Sc and Cu-Zr nanoglasses revealed that the Young's moduli of the nanoglasses are only 43 % of their metallic glass counterparts (Arnold et al., 2020). The lower values of the Young's moduli of the nanoglasses were, however, mostly attributed to sample porosity.

The present study shows that the Young's modulus of a nanoglass can be about 3% lower than that of a homogenous metallic glass with identical chemical composition in fully dense nanoglass samples. Although ultrasonic measurements (Arnold et al., 2020), nanoindentation experiments (Franke et al., 2014) using $Fe_{90}Sc_{10}$ nanoglasses as well as present nanoindentation simulations of $Cu_{64}Zr_{36}$ nanoglasses univocally show that the nanoglass has a lower Young's modulus as compared to its metallic glass counterpart, the difference exhibits large variations, which are due to different processing and testing conditions.

Finally, our simulations also reveal that plastic deformation is homogeneous in the as-prepared nanoglasses, while in the annealed nanoglasses it is a mix of shear bands and homogeneous deformation. Moreover, the plastic deformation in the nanoglasses is related to the degree of structural ordering in the interfaces. The homogeneous deformation in the as-prepared nanoglasses is consistent with scanning electron micrographs of indents in $Cu_{60}Zr_{40}$ nanoglasses (Sharma et al., 2021). However, the same experimental study reported that the plastic deformation in $Pd_{80}Si_{20}$ nanoglasses is carried by finer multiple secondary shear bands in addition to primary shear bands (Sharma et al., 2021). This deformation behavior is similar to that in the annealed nanoglasses presented in the current study. In fact, Nandam et al. (2020) have shown that $Pd_{80}Si_{20}$ simulated nanoglasses need to be annealed in order to make a direct comparison between experiment and simulation.

5. CONCLUSIONS

We have performed molecular dynamics simulations of nanoindentation in order to investigate the effects of segregation and structural relaxation on the mechanical properties of $Cu_{64}Zr_{36}$ nanoglasses prepared by particle consolidation. The glass-glass interfaces of these nanoglasses are characterized by a different composition and a defective short range order as compared the grain interiors. Our results show that annealing

of as-prepared nanoglasses at a temperature of 600 K ($\approx 0.8T_g$) for 500 ns induces structural relaxation which occurs mainly in the interfacial regions. The defective short–range order is not fully recovered after structural relaxation, suggesting that the microstructure of the nanoglass still exists even after annealing. The present findings show clearly that the effective elastic modulus of the nanoglass is lower than that of its homogeneous glass counterpart; this is because of the lower degree of ordering (i.e., the lower fraction of icosahedra) in the interfacial regions. Structural relaxation leads to a change of the deformation mode from homogeneous deformation to a mix of homogeneous deformation and shear bands. These findings demonstrate that the mechanical properties of nanoglasses are mainly controlled by the structural state of the interfaces, while in our model system chemical segregation to the interfaces influences only slightly the mechanical properties of as-prepared and annealed nanoglasses.

DATA AVAILABILITY STATEMENT

The raw data supporting the conclusions of this article will be made available by the authors, without undue reservation.

AUTHOR CONTRIBUTIONS

OA and KA: contributed the conception and design of the study. OA: setup and run the simulations, performed the analysis, and wrote the first draft of the manuscript. KA: supervision, review, and editing. Both authors contributed to the article and approved the submitted version.

FUNDING

The authors acknowledge the financial support of the Deutsche Forschungsgemeinschaft (DFG) through project Grant AL 578/15-2.

ACKNOWLEDGMENTS

The authors gratefully acknowledge the Gauss Centre for Supercomputing e.V. (www.gauss-centre.eu) for funding this project by providing computing time through the John von Neumann Institute for Computing (NIC) on the GCS Supercomputer JUWELS at Jülich Supercomputing Centre (JSC). Computational time was also made available by the Lichtenberg High Performance Computer Cluster at TU Darmstadt.

REFERENCES

Adibi, S., Sha, Z. D., Branicio, P. S., Joshi, S. P., Liu, Z. S., and Zhang, Y. W. (2013). A transition from localized shear banding to homogeneous superplastic flow in nanoglass. *Appl. Phys. Lett*. 103:211905. doi: 10.1063/1.4833018

Adjaoud, O., and Albe, K. (2016). Interfaces and interphases in nanoglasses: surface segregation effects and their implications on structural properties. *Acta Mater*. 113, 284–292. doi: 10.1016/j.actamat.2016.05.002

Adjaoud, O., and Albe, K. (2018). Microstructure formation of metallic nanoglasses: Insights from molecular dynamics simulations. *Acta Mater*. 145, 322–330. doi: 10.1016/j.actamat.2017.12.014

Adjaoud, O., and Albe, K. (2019). Influence of microstructural features on the plastic deformation behavior of metallic nanoglasses. *Acta Mater*. 168, 393–400. doi: 10.1016/j.actamat.2019.02.033

Adjaoud, O., and Albe, K. (2020). Mechanical properties of glassy nanopillars: a comparative, computational study of size effects in nanoglasses and homogeneous bulk glasses. *Front. Mater*. 7:352. doi: 10.3389/fmats.2020.544660

Albe, K., Ritter, Y., and Şopu, D. (2013). Enhancing the plasticity of metallic glasses: shear band formation, nanocomposites and nanoglasses investigated by molecular dynamics simulations. *Mech. Mater*. 67, 94–103. doi: 10.1016/j.mechmat.2013.06.004

Argon, A. (1979). Plastic deformation in metallic glasses. *Acta Metall*. 27, 47–58. doi: 10.1016/0001-6160(79)90055-5

Arnold, W., Birringer, R., Braun, C., Gleiter, H., Hahn, H., Nandam, S. H., et al. (2020). Elastic moduli of nanoglasses and melt-spun metallic glasses by ultrasonic time-of-flight measurements. *Trans. Indian Inst. Metals* 73, 1363–1371. doi: 10.1007/s12666-020-01969-x

Cheng, B., and Trelewicz, J. R. (2019a). Controlling interface structure in nanoglasses produced through hydrostatic compression of amorphous nanoparticles. *Phys. Rev. Mater*. 3:035602. doi: 10.1103/PhysRevMaterials.3.035602

Cheng, B., and Trelewicz, J. R. (2019b). Interfacial plasticity governs strain delocalization in metallic nanoglasses. *J. Mater. Res*. 34, 2325–2336. doi: 10.1557/jmr.2019.101

Cheng, Y., Cao, A., and Ma, E. (2009). Correlation between the elastic modulus and the intrinsic plastic behavior of metallic glasses: the roles of atomic configuration and alloy composition. *Acta Mater*. 57, 3253–3267. doi: 10.1016/j.actamat.2009.03.027

Cheng, Y., Cao, A., Sheng, H., and Ma, E. (2008). Local order influences initiation of plastic flow in metallic glass: effects of alloy composition and sample cooling history. *Acta Mater*. 56, 5263–5275. doi: 10.1016/j.actamat.2008.07.011

Cheng, Y. Q., Ding, J., and Ma, E. (2013). Local topology vs. atomic-level stresses as a measure of disorder: correlating structural indicators for metallic glasses. *Mater. Res. Lett*. 1, 3–12. doi: 10.1080/21663831.2012.722759

Choi, I. C., Zhao, Y., Kim, Y. J., Yoo, B. G., Suh, J. Y., Ramamurty, U., et al. (2012). Indentation size effect and shear transformation zone size in a bulk metallic glass in two different structural states. *Acta Mater*. 60, 6862–6868. doi: 10.1016/j.actamat.2012.08.061

Deng, C., and Schuh, C. A. (2012). Atomistic mechanisms of cyclic hardening in metallic glass. *Appl. Phys. Lett*. 100:251909. doi: 10.1063/1.4729941

Ding, J., Cheng, Y. Q., and Ma, E. (2014). Full icosahedra dominate local order in $Cu_{64}Zr_{36}$ metallic glass and supercooled liquid. *Acta Mater*. 69, 343–354. doi: 10.1016/j.actamat.2014.02.005

Falk, M. L., and Langer, J. S. (1998). Dynamics of viscoplastic deformation in amorphous solids. *Phys. Rev. E* 57, 7192–7205. doi: 10.1103/PhysRevE.57.7192

Fang, J. X., Vainio, U., Puff, W., Würschum, R., Wang, X. L., Wang, D., et al. (2012). Atomic structure and structural stability of $Sc_{75}Fe_{25}$ nanoglasses. *Nano Lett*. 12, 458–63. doi: 10.1021/nl2038216

Franke, O., Leisen, D., Gleiter, H., and Hahn, H. (2014). Thermal and plastic behavior of nanoglasses. *J. Mater. Res*. 29, 1210–1216. doi: 10.1557/jmr.2014.101

Gleiter, H. (2008). Our thoughts are ours, their ends none of our own: are there ways to synthesize materials beyond the limitations of today? *Acta Mater*. 56, 5875–5893. doi: 10.1016/j.actamat.2008.08.028

Gleiter, H. (2013). Nanoglasses: a new kind of noncrystalline materials. *Beilstein J. Nanotechnol*. 4, 517–533. doi: 10.3762/bjnano.4.61

Gleiter, H. (2016). Nanoglasses: a new kind of noncrystalline material and the way to an age of new technologies? *Small* 12, 2225–2233. doi: 10.1002/smll.201500899

Gleiter, H., Schimmel, T., and Hahn, H. (2014). Nanostructured solids–from nano-glasses to quantum transistors. *Nano Today* 9, 17–68. doi: 10.1016/j.nantod.2014.02.008

Ivanisenko, Y., Kübel, C., Nandam, S. H., Wang, C., Mu, X., Adjaoud, O., et al. (2018). Structure and properties of nanoglasses. *Adv. Eng. Mater*. 20:1800404. doi: 10.1002/adem.201800404

Jing, J., Krämer, A., Birringer, R., Gleiter, H., and Gonser, U. (1989). Modified atomic structure in a Pd-Fe-Si nanoglass. *J. Non Cryst. Solids* 113, 167–170. doi: 10.1016/0022-3093(89)90007-0

Kalcher, C., Adjaoud, O., and Albe, K. (2020). Creep deformation of a Cu-Zr nanoglass and interface reinforced nanoglass-composite studied by molecular dynamics simulations. *Front. Mater*. 7:223. doi: 10.3389/fmats.2020.00223

Kalcher, C., Adjaoud, O., Rohrer, J., Stukowski, A., and Albe, K. (2017a). Reinforcement of nanoglasses by interface strengthening. *Scripta Mater*. 141, 115–119. doi: 10.1016/j.scriptamat.2017.08.004

Kalcher, C., Brink, T., Rohrer, J., Stukowski, A., and Albe, K. (2017b). Interface-controlled creep in metallic glass composites. *Acta Mater*. 141, 251–260. doi: 10.1016/j.actamat.2017.08.058

Lee, J. C., Park, K. W., Kim, K. H., Fleury, E., Lee, B. J., Wakeda, M., et al. (2007). Origin of the plasticity in bulk amorphous alloys. *J. Mater. Res*. 22, 3087–3097. doi: 10.1557/JMR.2007.0382

Lee, K. S., Eckert, J., Jun, H. J., and Chang, Y. W. (2007). Influence of annealing on structural relaxation, crystallization, and deformation behavior of a $Zr_{41.2}Ti_{13.8}Cu_{12.5}Ni_{10}Be_{22.5}$ bulk metallic glass. *J. Mater. Res*. 22, 1849–1858. doi: 10.1557/jmr.2007.0253

Lee, S. W., Jafary-Zadeh, M., Chen, D. Z., Zhang, Y. W., and Greer, J. R. (2015). Size effect suppresses brittle failure in hollow $Cu_{60}Zr_{40}$ metallic glass nanolattices deformed at cryogenic temperatures. *Nano Lett*. 15, 5673–5681. doi: 10.1021/acs.nanolett.5b01034

Mendelev, M., Kramer, M., Ott, R., Sordelet, D., Yagodin, D., and Popel, P. (2009). Development of suitable interatomic potentials for simulation of liquid and amorphous Cu-Zr alloys. *Philos. Mag*. 89, 967–987. doi: 10.1080/14786430902832773

Nandam, S. H., Adjaoud, O., Schwaiger, R., Ivanisenko, Y., Chellali, M. R., Wang, D., et al. (2020). Influence of topological structure and chemical segregation on the thermal and mechanical properties of Pd–Si nanoglasses. *Acta Mater*. 193, 252–260. doi: 10.1016/j.actamat.2020.03.021

Nandam, S. H., Ivanisenko, Y., Schwaiger, R., Śniadecki, Z., Mu, X., Wang, D., et al. (2017). Cu-Zr nanoglasses: atomic structure, thermal stability and indentation properties. *Acta Mater*. 136, 181–189. doi: 10.1016/j.actamat.2017.07.001

Oliver, W., and Pharr, G. (2004). Measurement of hardness and elastic modulus by instrumented indentation: advances in understanding and refinements to methodology. *J. Mater. Res*. 19, 3–20. doi: 10.1557/jmr.2004.19.1.3

Plimpton, S. (1995). Fast parallel algorithms for short-range molecular dynamics. *J. Comput. Phys*. 117, 1–19. doi: 10.1006/jcph.1995.1039

Ritter, Y., Şopu, D., Gleiter, H., and Albe, K. (2011). Structure, stability and mechanical properties of internal interfaces in $Cu_{64}Zr_{36}$ nanoglasses studied by MD simulations. *Acta Mater*. 59, 6588–6593. doi: 10.1016/j.actamat.2011.07.013

Schuh, C. A., Hufnagel, T. C., and Ramamurty, U. (2007). Mechanical behavior of amorphous alloys. *Acta Mater*. 55, 4067–4109. doi: 10.1016/j.actamat.2007.01.052

Sharma, A., Nandam, S. H., Hahn, H., and Prasad, K. E. (2021). On the differences in shear band characteristics between a binary Pd-Si metallic and nanoglass. *Scripta Mater*. 191, 17–22. doi: 10.1016/j.scriptamat.2020.09.009

Shi, Y., and Falk, M. L. (2007). Stress-induced structural transformation and shear banding during simulated nanoindentation of a metallic glass. *Acta Mater*. 55, 4317–4324. doi: 10.1016/j.actamat.2007.03.029

Shimizu, F., Ogata, S., and Li, J. (2007). Theory of shear banding in metallic glasses and molecular dynamics calculations. *Mater. Trans*. 48, 2923–2927. doi: 10.2320/matertrans.MJ200769

Şopu, D., and Albe, K. (2015). Influence of grain size and composition, topology and excess free volume on the deformation behavior of Cu-Zr nanoglasses. *Beilstein J. Nanotechnol*. 6, 537–545. doi: 10.3762/bjnano.6.56

Şopu, D., Albe, K., Ritter, Y., and Gleiter, H. (2009). From nanoglasses to bulk massive glasses. *Appl. Phys. Lett*. 94:191911. doi: 10.1063/1.3130209

Şopu, D., Ritter, Y., Gleiter, H., and Albe, K. (2011). Deformation behavior of bulk and nanostructured metallic glasses studied via molecular dynamics simulations. *Phys. Rev. B* 83:100202. doi: 10.1103/PhysRevB.83.100202

Stukowski, A. (2010). Visualization and analysis of atomistic simulation data with OVITO-the open visualization tool. *Model. Simul. Mater. Sci. Eng*. 18:015012. doi: 10.1088/0965-0393/18/1/015012

Tang, C., and Harrowell, P. (2013). Anomalously slow crystal growth of the glass-forming alloy CuZr. *Nat. Mater*. 12, 507–511. doi: 10.1038/nmat3631

Wang, C., Wang, D., Mu, X., Goel, S., Feng, T., Ivanisenko, Y., et al. (2016). Surface segregation of primary glassy nanoparticles of $Fe_{90}Sc_{10}$ nanoglass. *Mater. Lett*. 181, 248–252. doi: 10.1016/j.matlet.2016.05.189

Wang, X., Jiang, F., Hahn, H., Li, J., Gleiter, H., Sun, J., et al. (2016). Sample size effects on strength and deformation mechanism of $Sc_{75}Fe_{25}$ nanoglass and metallic glass. *Scripta Mater*. 116, 95–99. doi: 10.1016/j.scriptamat.2016.01.036

Wang, X. L., Jiang, F., Hahn, H., Li, J., Gleiter, H., Sun, J., et al. (2015). Plasticity of a scandium-based nanoglass. *Scripta Mater*. 98, 40–43. doi: 10.1016/j.scriptamat.2014.11.010

Weissmüller, J., Birringer, R., and Gleiter, H. (1992). Nanostructured crystalline and amorphous solids. *Key Eng. Mater*. 77–78, 161–170. doi: 10.4028/www.scientific.net/KEM.77-78.161

Yoo, B. G., Park, K. W., Lee, J. C., Ramamurty, U., and Jang, J. I. (2009). Role of free volume in strain softening of as-cast and annealed bulk metallic glass. *J. Mater. Res*. 24, 1405–1416. doi: 10.1557/jmr.2009.0167

Zemp, J., Celino, M., Schönfeld, B., and Löffler, J. F. (2015). Crystal-like rearrangements of icosahedra in simulated copper-zirconium metallic glasses and their effect on mechanical properties. *Phys. Rev. Lett*. 115:165501. doi: 10.1103/PhysRevLett.115.165501

Conflict of Interest: The authors declare that the research was conducted in the absence of any commercial or financial relationships that could be construed as a potential conflict of interest.